Solvation Structures and Dynamics of Magnesium Chloride (Mg2+-Cl-) Ion-Pair in Water-Ethanol Mixtures.

ARTICLE *in* THE JOURNAL OF PHYSICAL CHEMISTRY A · JULY 2013

Impact Factor: 2.69 · DOI: 10.1021/jp4031706 · Source: PubMed

3 AUTHORS, INCLUDING:

Anupam Chatterjee
Indian Institute of Technology Bombay
1 PUBLICATION **8** CITATIONS
SEE PROFILE

Mayank Kumar Dixit
Indian Institute of Technology Bombay
11 PUBLICATIONS **18** CITATIONS
SEE PROFILE

THE JOURNAL OF PHYSICAL CHEMISTRY A

Article

pubs.acs.org/JPCA

Solvation Structures and Dynamics of the Magnesium Chloride (Mg^{2+}–Cl^{-}) Ion Pair in Water–Ethanol Mixtures

Anupam Chatterjee,[†] Mayank Kumar Dixit,[†] and B. L. Tembe*

Department of Chemistry, Indian Institute of Technology, Bombay, Powai, Mumbai 400076, India

Supporting Information

ABSTRACT: We have performed constrained molecular dynamics simulations of magnesium chloride in water–ethanol mixtures. From the potentials of mean force (PMFs) of the Mg^{2+}–Cl^{-} ion pair, we notice that, as the mole fraction of ethanol increases, the depths of the minima of the contact ion pair (CIP) and solvent assisted ion pair (SAIP) increase, but the depth of the CIP minimum increases more in comparison to the SAIP minimum. This shows that ion pairing becomes more favorable with an increase in the mole fraction of ethanol. Significant differences in the PMFs between the Mg^{2+} and the Cl^{-} ion (depending upon whether the second Cl^{-} ion is present in the first coordination shell of the Mg^{2+} ion or not) seem to have been reported for the first time in this work. The local mole fraction of water molecules in the first solvation shell of ions is generally greater than in the bulk. The diffusional behavior of solvent molecules in solvation shells of the ion-pair indicates that the ions as well as the first solvation shells of the ions diffuse at much slower rates. Also, the diffusion constant of bulk water in the mixtures is greatly reduced compared to the pure solvent value.

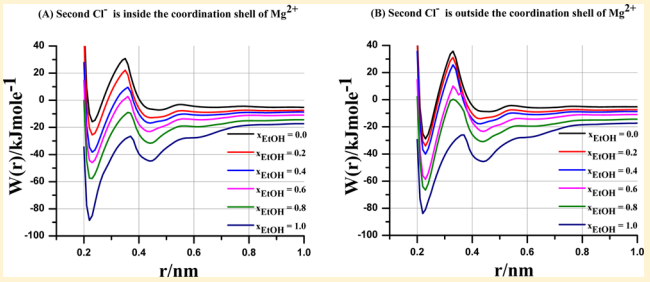

1. INTRODUCTION

Aqueous solutions of $MgCl_2$ play a significant role in biological and environmental systems. Magnesium ion stabilizes the structure of DNA, RNA, proteins, and cell membranes.[1−4] The magnesium ion works as a catalyst in enzymes. Some biological reactions occur at high pH, but in the presence of Mg^{2+}, these reaction occur at biological pH.[1] Magnesium ion as well as fully hydrated magnesium dication can interact with protein molecules.[1−4] Metal–RNA interactions play a crucial role in the folding of RNA.[5,6] Magnesium dication is bound to RNA in the crystals of Hepatitis delta virus (HDV). In the presence of magnesium dication, the cleavage reaction occurs in crystals of Hepatitis delta virus (HDV).[7] After sodium chloride, magnesium chloride is the next most distinguished inorganic salt found in seawater.[8]

The solvation structures of $MgCl_2$ in aqueous solution have been studied[9−15] with the help of classical molecular dynamics simulations. The hydration structure of Mg^{2+} has been investigated by many first principal molecular dynamics and Monte Carlo simulations.[16−21] It is observed from studies of solvation structures of magnesium chloride using ab initio molecular dynamics, density functional theory, and Car–Parrinello molecular dynamics (CPMD) that in the first solvation shell of magnesium ion there are six water molecules arranged in an octahedral arrangement around magnesium ion and the radius of first solvation shell ranges from 2.01 to 2.13 Å.[22−30]

Many chemical as well as biological reactions are studied in water–ethanol mixtures. Franks and Ives noted that water–alcohol mixtures are used in the investigation of complex systems.[31] The abnormal behavior of water–ethanol mixtures are observed in negative partial molar volume,[32,33] heats of solution,[34] and the chemical shift of hydrogen of water.[35,36] In water–ethanol mixtures, even a small amount of alcohol can enhance the hydrogen bonding association among water molecules.[36]

A number of studies have been done on water–ethanol mixtures.[37,38] Chun et al.[37] have studied the adsorption mechanism of water and ethanol inside gold nanotubes. They have shown that the interaction between water molecules and the Au nanotubes is stronger than that between ethanol molecules and Au nanotubes. The solutions of guanidinium chloride in a water–ethanol mixture are commonly used to denature macromolecules such as proteins and DNA.[38] The diffusion coefficients of guanidinium chloride in water–ethanol mixtures have been calculated.[38] Diffusion of guanidinium chloride is useful in the study of unfolding of macromolecules.[39,40]

The classical molecular dynamics simulations of $MgCl_2$ and $CaCl_2$ in water–methanol mixtures have been performed and it has been observed that cations are preferentially solvated by water molecules and chloride ions are preferentially solvated by methanol molecules.[41] The solution of $MgCl_2$ in water–ethanol

Special Issue: Structure and Dynamics: ESDMC, IACS-2013

Received: March 31, 2013
Revised: July 5, 2013

   dx.doi.org/10.1021/jp4031706 | J. Phys. Chem. A XXXX, XXX, XXX–XXX

Table 1. Details of the Simulation Boxes of the Mixtures

no.	x_{EtOH}	x_{H2O}	n_{EtOH}	n_{H2O}	L (Å)	ρ(g mL^{-1})	ε
1	0.0	1.0	0	1000	31.10	994.3 ± 0.2	53.0 ± 0.9
2	0.206	0.794	156	600	34.10	925.7 ± 0.3	37.2 ± 0.5
3	0.370	0.630	235	400	34.60	886.4 ± 0.4	31.9 ± 0.5
4	0.610	0.390	313	200	34.42	843.8 ± 0.4	25.3 ± 0.2
5	0.779	0.221	352	100	34.15	820.4 ± 0.3	19.3 ± 0.5
6	1.0	0.0	391	0	33.60	792.7 ± 0.4	16.0 ± 0.5

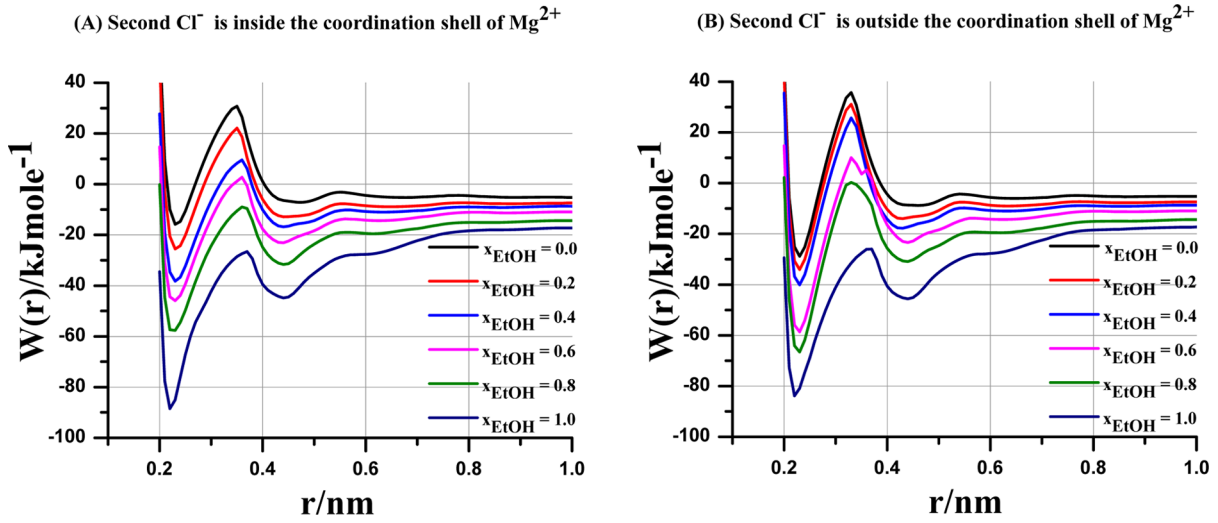

Figure 1. Potentials of mean force (PMFs) of $Mg^{2+}Cl^{-}$ ion pair in EtOH–water mixtures from 0 to 1.0 ethanol mole fraction when the second Cl^{-} ion is (A) inside and (B) outside the coordination shell of Mg^{2+} ion.

mixtures is an important area for investigation. To understand the preferential solvation and diffusional behavior of magnesium and chloride ions, we have performed constrained molecular dynamics simulation of $MgCl_2$ in water–ethanol mixtures.

2. METHODOLOGY AND COMPUTATIONAL DETAILS

All MD simulations were done using the GROMACS package (version 4.5.4).[42] The united atom optimized potentials for liquid simulation (OPLS) force fields[43] have been used for ethanol and magnesium chloride ion pairs. TIP4P model[44] is used for water molecules. Earlier simulations indicated that the TIP4P model of water reproduces the excess mixing properties in water–methanol mixtures rather well.[45]

The solvent–solvent, solvent–solute, and solute–solute interactions are taken to be pairwise additive and composed of the Lenard-Jones and Columbic terms

$$U_{\alpha\beta} = \left(\frac{A_{\alpha\beta}}{r^{12}} - \frac{B_{\alpha\beta}}{r^{6}}\right) + \frac{q_\alpha q_\beta}{r} \quad (1)$$

where α and β denote a pair of interactions sites on different molecules, r is the site–site separation, q_α is charge located at site α, and q_β is the charge located at site β. The terms $A_{\alpha\beta}$ and $B_{\alpha\beta}$ are determined from

$$A_{\alpha\beta} = 4\varepsilon_{\alpha\beta}(\sigma_{\alpha\beta})^{12} \quad (2)$$

$$B_{\alpha\beta} = 4\varepsilon_{\alpha\beta}(\sigma_{\alpha\beta})^{6} \quad (3)$$

whereas $\varepsilon_{\alpha\beta}$, $\sigma_{\alpha\beta}$ are calculated using the following mixing rules.

$$\varepsilon_{\alpha\beta} = (\varepsilon_{\alpha\alpha}\cdot\varepsilon_{\beta\beta})^{1/2} \quad (4)$$

$$\sigma_{\alpha\beta} = (\sigma_{\alpha\alpha}\cdot\sigma_{\beta\beta})^{1/2} \quad (5)$$

The potential of mean force, $W(r)$ of the ion pair in the presence of the solvent can then be calculated as

$$W(r) = -\int F(r)\,dr = W(r_0) - \int_{r_0}^{r} F(r)\,dr \quad (6)$$

$$W(r_0) = \frac{q_i q_j}{\varepsilon r_0} \quad (7)$$

where $F(r)$ is the mean force between the ion pair at distance r. The distance r is varied from 2.0 to 10.0 Å with increments of 0.1 Å. The value of r_0 is 10.0 Å for all compositions and ε is the dielectric constant of the mixture.

We have used particle mesh Ewald electrostatics[46] with a direct space cutoff of 1.0 nm and a grid spacing of 0.12 nm. For nonbonded van der Waals interactions, a 1.5 nm cutoff was used. The geometry of water and ethanol molecules was maintained during the simulations by using the SHAKE[47] algorithm. The temperature of the system is 298 K and it was kept constant using the velocity rescaling thermostat.[48] The details of the chosen solvent mixtures are given in Table 1.

We have used packmole[49] to generate the initial configurations of all the systems. All systems were equilibrated for 2 ns by performing *NPT* simulations using Brendsen pressure coupling.[50] For generating the trajectories we have performed longer NPT simulations (6 ns) by using Parrinello–Rahman pressure coupling.[51,52] The integration time step was 2 fs. The mean forces between the ions were calculated for distances ranging from 2 to 10.0 Å for calculating the PMFs and the PMFs are further confirmed by constraint free molecular dynamics.

dx.doi.org/10.1021/jp4031706 | J. Phys. Chem. A XXXX, XXX, XXX–XXX

3. RESULTS AND DISCUSSION

3.1. Potentials of Mean Force. We have observed in our simulations that the solvation structure of the Mg^{2+}−Cl^- ion pair depends upon whether the second Cl^- is present in solvation shell of Mg^{2+} or it is present in the bulk, away from the ion pair. To understand these solvation structures, we have done two sets of simulations, namely (i) the second Cl^- is present in solvation shell of Mg^{2+} and (ii) the second Cl^- is present in the bulk.

Figure 1 shows the potentials of mean force of the Mg^{2+}−Cl^- ion pair in water−ethanol mixtures with x_{EtOH} = 0.0, 0.2, 0.4, 0.6, 0.8, and 1.0 when the second Cl^- ion is inside (Figure 1A) and outside the Mg^{2+} hydration shell (Figure 1B). From Figure 1A, it is observed that, in each curve, there are two minima. The first minimum represents the contact ion pair (CIP), and second minimum represents the solvent assisted ion pair (SAIP). In each mixture, the position of CIP is around 2.3 Å and the position of SAIP is in between 4 and 5 Å. In each composition of water−ethanol mixtures, the depth of the CIP minimum is more than the depth of the SAIP minimum. This shows that contact ion pair is more stable than solvent assisted ion pair in each composition of water−ethanol mixtures.

As the mole fraction of ethanol increases, the depths of the CIP minima as well as SAIP minima generally increase. Therefore, CIPs and SAIPs become more stable with increase in the mole fraction of ethanol. There is a significant decrease (of 32 kJ mol^{-1}) in the depth of the CIP minimum as compared to the SAIP minimum when the mole fraction of water increases from 0 to 0.2 in the case of PMFs when the second chloride is in the Mg^{2+} shell.

In Figure 1B, the free Cl^- ion is outside the Mg^{2+} hydration shell. We note here the differences between Figure 1A,B. The CIPs in Figure 1A are more stable than the CIPs in Figure 1B for x_{EtOH} = 1. Between panels A and B of Figure 1, the main differences are in the changes in the depths of CIPs. For the case where the second Cl^- is inside the Mg^{2+} shell (Figure 1A), the depths of the CIPs change from −88 to −16 $kJmol^{-1}$. For the other case (Figure 1B), the depths change from −84 to −29 $kJmol^{-1}$. For all other compositions (other than x_{EtOH} = 1), the depths of the CIPs are greater and the heights of the transition states higher for the case when the second Cl^- is in the bulk. Separate PMFs for each composition for the two cases (for second Cl^- in the Mg^{2+} shell and in the bulk) are given in Figure S1 in the Supporting Information. This is caused by the second Cl^- in the Mg^{2+} shell, which attracts more water molecules in the Mg^{2+} shell. This is the main role of the second Cl^- inside the solvation shell on the CIP depths and transition state heights. The simulation error bars in each curve are in the range of 1 $kJmol^{-1}$.

3.2. Residence Times of the Ion Pairs. An additional confirmation of the potentials of mean force of the Mg^{2+}−Cl^- ion pair comes from the residence times of the ion pair at various ion−ion separations. The residence times have been calculated by performing dynamical trajectories of the ion pair initiated at different ion−ion separations. This is done by performing long MD simulations on systems by releasing the constraint on the ion pair and then calculating the ion−ion separation vector at each time step. We have taken several interionic separations (in the range 2.0−8.0 Å) as initial ion−ion distances, and each trajectory is evolved for 1 ns. The residence times for each ion pair are averaged over 40 trajectories for each composition. We have calculated the residence times for the Mg^{2+}−Cl^- ion pair for all water−ethanol mixtures. These are shown in Figure 2. Curves a−f refer to different values of x_{EtOH}.

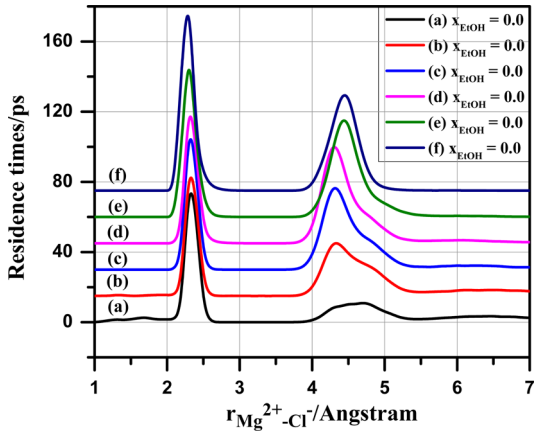

Figure 2. Residence times of the Mg^{2+}−Cl^- ion pair in EtOH−water mixtures. The mole fraction of ethanol ranges from 0 to 1.0. Each curve is over a 1 ns simulation with several trajectories initiated at different initial values of $r_{Mg^{+2}-Cl^-}$ in the range 2−8 Å. Curves b−f are shifted upward from curve a (for clarity) by 15, 30, 45, 60, and 75 units, respectively.

It is clear from Figure 2 that in each curve, there are two peaks: the intense peak corresponds to contact ion pair, and the broad peak corresponds to solvent assisted ion pair. As the mole fraction of ethanol increases, the intensity of the broad peak increases. This shows that, as the mole fraction of ethanol increases, the stability of SAIPs increases.

3.3. Solvation Structure of the Ion Pair. We now analyze the effect of composition on the solvation structure around the ion pair at different separations of the ion pair. For this purpose, we calculate the running coordination numbers (RCNs) around the ions with the help of eq 8 in all water−ethanol mixtures. The coordination number is defined as[53]

$$n_{\alpha\beta} = 4\pi\rho_\beta \int_{r_1}^{r_2} r^2 g_{\alpha\beta}(r)\, dr \tag{8}$$

where $n_{\alpha\beta}$ represents the number of atoms of type β surrounding species α in a shell extending from r_1 to r_2, ρ_β is the number density of β in the system, and $g_{\alpha\beta}(r)$ is the radial distribution function (which gives the ratio of local mole fraction of β and the bulk mole fraction of β) for the site β around site α. For the calculation of the first solvation shell coordination number, the value of r_1 is zero and the value of r_2 is the first minimum in the radial distribution function.

The local mole fraction of solvent molecules of type i, in the first solvation shell around ions (s) is defined as[54]

$$x_i^L(s,R_a) = \frac{\rho_i \int_0^{R_a} g_{is}(R) 4\pi R^2\, dR}{\sum_{j=1}^{c} \rho_j \int_0^{R_a} g_{js}(R) 4\pi R^2\, dR} \tag{9}$$

where ρ_i is the number density of solvent molecules of type i, $g_{is}(R)$ is correlation function between ions (s) and solvent molecules of type (i), R_a is the position of first minima in the radial distribution function, and c is the number of components present in the system.

In Figure 3, the local mole fractions of ethanol and water molecules in first coordination shell around the Mg^{2+} and Cl^-

dx.doi.org/10.1021/jp4031706 | J. Phys. Chem. A XXXX, XXX, XXX−XXX

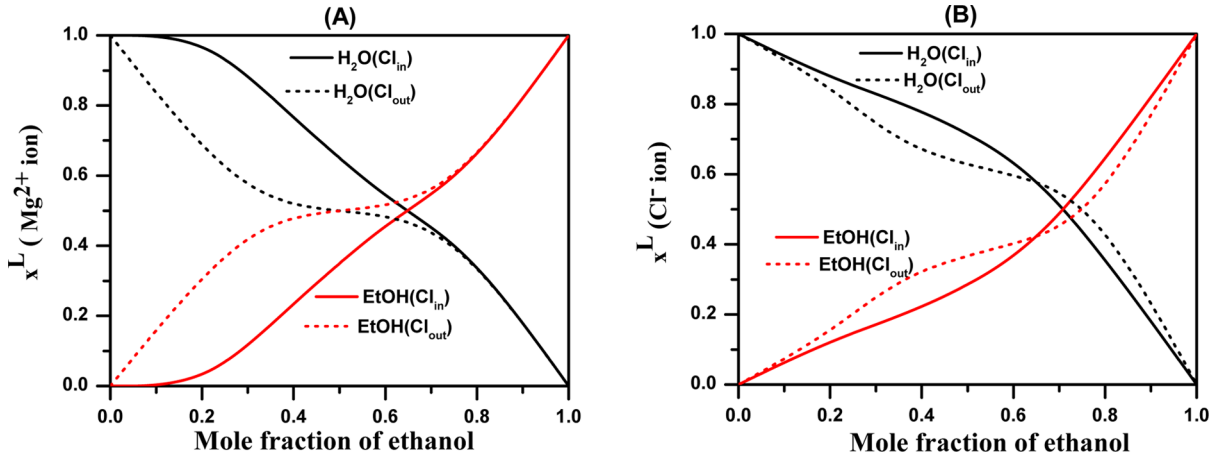

Figure 3. Local mole fractions of solvent molecules in the first coordination shell of (A) the Mg^{2+} ion and (B) the Cl^- ion of the ion pair. Solid lines represent the case when the second Cl^- ion is inside the coordination shell of Mg^{2+}, and dashed lines represent the case when the second Cl^- ion is in the bulk, i.e, outside the coordination shell of Mg^{2+}.

ions in the SAIP state are shown at different mole fractions of ethanol. The black lines (solid and dashed) represent the local mole fraction of water molecules in the first coordination shell around the ions. The red lines (solid and dash) represent the local mole fraction of ethanol molecules in the first coordination shell around the ions. Solid lines represent the case when the second Cl^- ion is inside the coordination shell of Mg^{2+}, and dashed lines represent second Cl^- ion is outside the coordination shell of Mg^{2+}. It is observed from Figure 3B that there is preferential solvation of chloride by water molecules in the entire composition range. When the second chloride moves from the Mg^{2+} shell to the bulk, the effects on the local mole fractions are of the order of 10% but do not change the nature of preferential solvation. In the case of Mg^{2+} (Figure 3A), the effects are striking in the mole fraction range x_{EtOH} = 0.0−0.5. In this mole fraction range, the preferential solvation of Mg^{2+} changes from ethanol dominant environment to water dominant environment. This is caused by the second Cl^- present in the Mg^{2+} shell, which attracts more water molecules into the first shell.

3.4. Diffusion Constants of Ion Pair, Coordination Shells, and Bulk Solvents in the Water−Ethanol Mixture.

We have studied the diffusion patterns of Mg^{2+} and Cl^- ions and other molecules in the solvation shell as well as the bulk solvent molecules.

The diffusion coefficients (D) were calculated from the mean square displacements, using the Einstein's relation

$$D = \frac{\langle |r_i(t + \Delta t) - r_i(t)|^2 \rangle}{6t} \quad (10)$$

where $r_i(t)$ is the position of the site i at time t.

Figure 4 shows the MSD plots for x_{EtOH} = 0. The MSDs for bulk water, shell water, the second Cl^- in the Mg^{2+} shell, Mg^{2+}, and the paired Cl^- of the ion pair are shown. It is observed from Figure 4 that the diffusional constants of solvent molecules in the solvation shells of the ion pair is much slower than the bulk solvent values. The diffusion constants of the Mg^{2+} ion, shell water, bulk water, shell ethanol, and bulk ethanol for all water−ethanol mixtures are given in Table 2.

The diffusion constants (D) of water and ethanol are 3.4 and 1.39 (all values of diffusion constants are in units of 10^{-5} cm^2 s^{-1}) for x_{EtOH} = 0.0 and 1.0, respectively. In the mixtures, the diffusion constants of bulk solvent molecules are lower than the

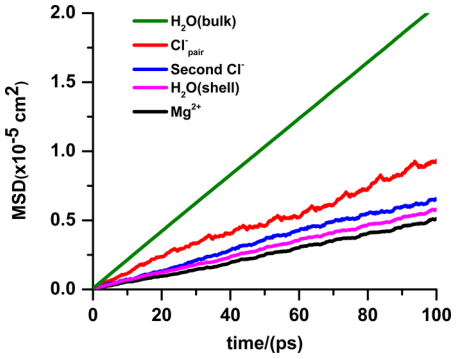

Figure 4. Mean square displacement versus time for the Mg^{2+} ion (black), the water molecules in the first coordination shell (pink), the second Cl^- (blue) present in the first coordination shell of magnesium, Cl^-_{pair} of the ion pair (red), and bulk water (green).

pure solvent cases. In the case of water, the value of D decreases to 1.15 for x_{EtOH} = 0.6 and 0.8. The values of D for both water and ethanol are very small in the solvation shells, ranging from one-fourth to one-third of the bulk values. The diffusion constants of the ions are even smaller than the D values of the solvation shell molecules. The differences in D values between the cases when the second Cl^- is in the coordination shell of Mg^{2+} or outside it are not very significant for water and ethanol in the solvation shells. Finally, we note that when the bound Cl^- (second) is removed from the solvation shell of Mg^{2+}, its D value (column 6 of Table 2) is more than the D value for the Cl^- associated with the ion pair (column 4 of Table 2).

Figure 5 (a) shows a representative snapshot of the first coordination shell of Mg^{2+} ion (green) contains four ethanol molecules at a CIP of Mg^{2+}−Cl^- in pure ethanol (second Cl^- inside the shell of Mg^{2+}). Figure 5 (b) shows that the first coordination shell of Mg^{2+} ion contains three ethanol molecules and a water molecule at a CIP, in water−ethanol mixture with x_{EtOH} = 0.8. Therefore, as we go from pure ethanol to water−ethanol mixture with x_{EtOH} = 0.8, one ethanol molecule is replaced by one water molecule. Due to this as well as due to the presence of the second Cl^-, there is a significant decrease in the depth of CIP minimum.

dx.doi.org/10.1021/jp4031706 | J. Phys. Chem. A XXXX, XXX, XXX−XXX

Table 2. Diffusion Coefficients (10^{-5} cm^2 s^{-1}) of Mg^{2+} and Cl^- of the Ion Pair, Free Cl^- (Second Cl^- Ion), Solvent Molecules in the Shell, and Solvent Molecules in the Bulk for All Compositions Mentioned on the Left[a]

	Mg^{2+} ion		Cl^- of ion pair		second Cl^-		H_2O in Mg^{2+} shell		H_2O in bulk	EtOH in Mg^{2+} shell		EtOH in bulk
system x_{EtOH}	A	B	A	B	A	B	A	B	A, B	A	B	A, B
0.0	0.79	0.60	2.60	2.40	0.83	2.75	1.10	0.82	3.40			
0.2	0.41	0.48	0.81	0.69	0.63	0.84	0.60	0.57	1.60		0.61	1.18
0.4	0.25	0.19	0.41	0.33	0.37	0.67	0.30	0.23	1.27	0.36	0.38	0.93
0.6	0.22	0.26	0.44	0.47	0.31	0.58	0.25	0.30	1.15	0.29	0.34	1.05
0.8	0.27	0.23	0.39	0.25	0.33	0.46	0.33	0.25	1.16	0.41	0.35	1.57
1.0	0.37	0.41	0.49	0.34	0.40	0.48				0.48	0.56	1.39

[a]Symbol A represents that the second Cl^- ion is inside and symbol B represents that the second Cl^- ion is outside the coordination shell of Mg^{2+} ion.

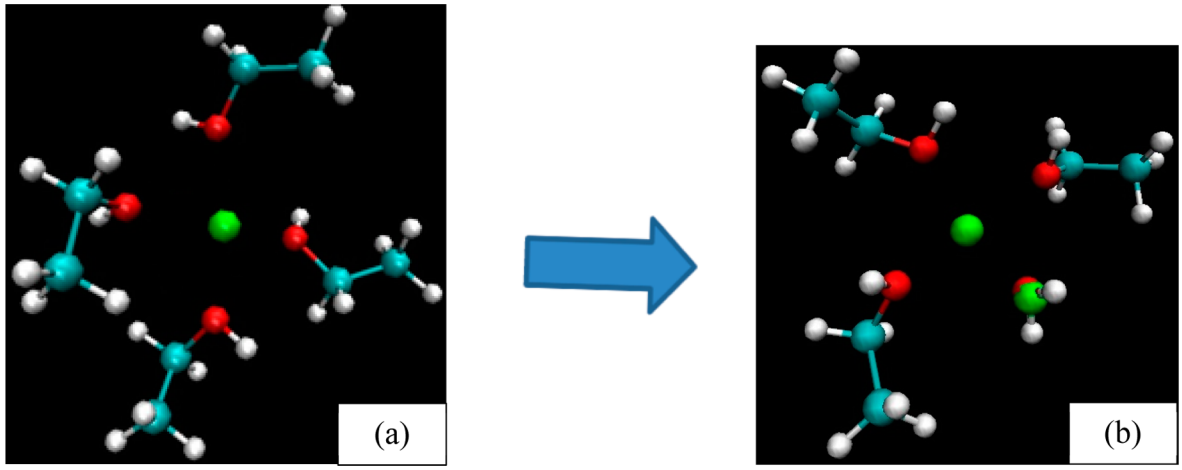

Figure 5. Representation of the snapshots of the contact ion pair for Mg^{2+}–Cl^- in (a) pure ethanol and (b) water–ethanol mixture with mole fraction of ethanol is 0.8.

4. CONCLUSIONS

We have performed constrained molecular dynamics simulations of magnesium chloride in water–ethanol mixtures. We observe that, as the mole fraction of ethanol increases, ion pairing becomes more favorable between Mg^{2+} and Cl^- ions. There is a sharp decrease in the depth of the CIP minima as compared to the SAIP minima in the mole fraction range of water between 0.0 and 0.20, especially when the second Cl^- is inside the Mg^{2+} shell. In the case when the second Cl^- is in the bulk, the CIP minima are deeper and the transition state maxima are also higher for all compositions other than x_{EtOH} = 1. These results are also confirmed from the data of the residence times of the ion pair at various inter-ion separations. The local mole fractions of the solvent and their running coordination numbers (RCNs) (Figure S5, given in the Supporting Information) show that a water molecule is in the coordination shell of Mg^{2+} even when the mole fraction of water in the bulk mixture is 0.2. The local mole fraction of water molecules in the first solvation shell of ions is generally greater than in the bulk. The diffusional behavior of the solvent molecules in the solvation shells of the ion pair indicates that the ions as well as the first solvation shells of the ions diffuse at rates which are about one-fourth one-third of the rate of the bulk solvent values. Also, the diffusion constant of bulk water in the mixtures is greatly reduced compared to the bulk pure solvent values.

■ ASSOCIATED CONTENT

Supporting Information

Separate PMFs of the Mg^{2+}–Cl^- ion pair for each composition for the two cases (for the second Cl^- in the Mg^{2+} shell and in the bulk). The radial distribution functions between Mg^{2+}–O_{wt} and Mg^{2+}–O_{EtOH} calculated at three ion–ion separations, i.e., CIPs, TS, and SAIPs, for two compositions with x_{EtOH} = 0.6, 0.8. Running coordination numbers around Mg^{2+} and Cl^- ions. This material is available free of charge via the Internet at http://pubs.acs.org.

■ AUTHOR INFORMATION

Corresponding Author

*Phone no.: +91-22-2576-4199. Fax no.: +91-22-2576-7152. E-mail: bltembe@chem.iitb.ac.in.

Notes

The authors declare no competing financial interest.

†E-mail: A.C., anupam.chatterjee@chem.iitb.ac.in; M.K.D., mayankd@chem.iitb.ac.in.

■ ACKNOWLEDGMENTS

We express our gratitude to IIT Bombay for providing us with the High performance Computing Facility and the Department of Chemistry, IIT Bombay, for providing research facilities. A.C. thanks the support received through the KVPY Fellowship funded by DST, Government of India. M.K.D. thanks UGC, Government of India, for a Senior Research Fellowship.

dx.doi.org/10.1021/jp4031706 | J. Phys. Chem. A XXXX, XXX, XXX–XXX

REFERENCES

(1) Cowan, J. A. Structural and Catalytic Chemistry of Magnesium-Dependent Enzymes. *Biometals* **2002**, *15*, 225−235.

(2) Jiao, D.; King, C.; Grossfield, A.; Darden, T. A.; Ren, P. Simulation of Ca^{2+} and Mg^{2+} Solvation Using Polarizable Atomic Multipole Potential. *J. Phys. Chem. B* **2006**, *110*, 18553−18559.

(3) Bernasconi, L.; Baerends, E. J.; Sprik, M. Long-Range Solvent Effects on the Orbital Ineraction Mechanism of Water Acidity Enhancement in Metal Ion Solutions: A Comparative Study of the Electronic Structure of Aqueous Mg and Zn Dications. *J. Phys. Chem. B* **2006**, *110*, 11444−11453.

(4) Gong, B.; Chen, Y.; Christian, E. L.; Chen, J.-H.; Chase, E.; Chadalavada, D. M.; Yajiima, R.; Golden, B. L.; Bevilacqua, P. C.; Carey, P. R. Detection of Innersphere Interations between Magnesium Hydrate and the Phophate Backbone of the HDV Ribozyme Using Raman Crystallography. *J. Am. Chem. Soc.* **2008**, *130*, 9670−9672.

(5) DeRose, V. J. Metal Ion Binding to Catalytic RNA Molecules. *Curr. Opin. Struct. Biol.* **2003**, *13*, 317−324.

(6) Sigel, R. K. O; Pyle, A. M. Alternative Roles for Metal Ions in Enzyme Catalysis and the Implications for Ribozymes Chemistry. *Chem. Rev.* **2007**, *107*, 97−113.

(7) Gong, B.; Chen, J. H.; Chase, E.; Chadalavada, D. M.; Yajima, R.; Golden, B. L.; Bevilacqua, P. C.; Carey, P. R. Direct Measurement of a pK_a near Neutrality for the Catalytic Cytosine in the Genomic HDV Ribozyme Using Raman Crystallography. *J. Am. Chem. Soc.* **2007**, *129*, 13335−13342.

(8) *CRC Handbook of Chemistry and Physics*, 77th ed.; CRC Press: Boca Raton, FL, 1996.

(9) Dietz, W.; Riede, W. O.; Heinzinger, K. The Structure of Aqueous Electrolytic Solutions As Derived from MD Simulation. *Z. Naturforsch.* **1982**, *37a*, 1038−1048.

(10) Bock, C.; Markham, G.; Katz, A.; Glusker, J. The Arrangement of First- and Second-Shell Water Molecules around Metal Ions: Effects of Charge and Size. *Theor. Chem. Acc.* **2006**, *115*, 100−112.

(11) Guardia, E.; Sese, G.; Padro, J. A.; Kalko, S. G. Molecular Dynamics Simulation of Mg^{2+} and Ca^{2+} Ions in Water. *J. Solution Chem.* **1999**, *28*, 1113−1126.

(12) Szasz, G. I.; Dietz, W.; Heinzinger, K.; Palinkas, G.; Radnai, T. On the Orientation of Water Molecules in the Hydration Shell of the Ions in a $MgCl_2$ Solution. *Chem. Phys. Lett.* **1982**, *92*, 388−392.

(13) Palinkas, G.; Radnai, T.; Dietz, W.; Szasz, G. I.; Heinzinger, K. Hydration Shell Structure in a Magnesium Chloride Solution from X-ray and MD Studies. *Z. Naturforsch.* **1982**, *37a*, 1049−1060.

(14) Heinzinger, K. Computer Simulations of Aqueous Electrolyte Solutions. *Physica* **1985**, *131B*, 196−216.

(15) Zapalowski, M.; Batczak, W. M. Concentrated Aqueous $MgCl_2$ Solutions. A Computer Simulation Study of the Solution Structure and Excess Electron Localisation. *Res. Chem. Intermed.* **2001**, *27*, 855−866.

(16) Lightstone, F. C.; Schwegler, E.; Hood, R. Q.; Gygi, F.; Galli, G. A first Principles Molecular Dynamics Simulation of the Hydrated Magnesium Ion. *Chem. Phys. Lett.* **2001**, *343*, 549−555.

(17) Krekeler, C.; Delle Site, L. Solvation of Positive Ions in Water: The Dominant Role of Water-Water Interaction. *J. Phys.: Condens. Matter* **2007**, *19*, 192101−192107.

(18) Tongraar, A.; Rode, B. M. Structural Arrangement and Dynamics of the Hydrated Mg^{2+}: An Ab Initio QM/MM Molecular Dynamics Simulation. *Chem. Phys. Lett.* **2005**, *409*, 304−309.

(19) Tongraar, A.; Rode, B. M. The Role of Non-Additive Contributions on the Hydration Shell Structure of Mg^{2+} Studied by Born-Oppenheimer Ab Initio Quantum Mechanical/Molecular Mechanical Molecular Dynamics Simulation. *Chem. Phys. Lett.* **2001**, *346*, 485−491.

(20) Ikeda, T.; Boero, M.; Terakura, K. Hydration Properties of Magnesium and Ions from Constrained First Principles Molecular Dynamics. *J. Chem. Phys.* **2007**, *127*, 074503−074508.

(21) Tofteberg, T.; Ohrn, A.; Karlstrom, G. Combined Quantum Chemical Statistical Mechanical Simulations of Mg^{2+}, Ca^{2+} and Sr^{2+} in Water. *Chem. Phys. Lett.* **2006**, *429*, 436−439.

(22) Markham, G. D.; Glusker, J. P.; Bock, C. L.; Trachtman, M.; Bock, C. W. Hydration Energies of Divalent Beryllium and Magnesium Ions: An ab Initio Molecular Orbital Study. *J. Phys. Chem.* **1996**, *100*, 3488−3497.

(23) Markham, G.; Glusker, J.; Bock, C. The Arrangment of First- and Second-Sphere Water Molecules in Divalent Magnesium Complexes: Resuilts from Molecular Orbital and Density Functional Theory and from Structural Crystallography. *J. Phys. Chem. B* **2002**, *106*, 5118−5134.

(24) Jagoda-Cwiklik, B.; Jungwirth, P.; Rulisek, L.; Milko, P.; Roithova, J.; Lemaire, J.; Maitre, P.; Ortega, J. M.; Schroder, D. Micro-Hydration of the $MgNO_3$ Cation in the Gas Phase. *Chem. Phys. Chem.* **2007**, *8*, 1629−1639.

(25) Bock, C.; Markham, G.; Katz, A.; Glusker, J. The Arrangement of First- And Second-Shell Water Molecules around Metal Ions: Effects of Charge and Size. *Theor. Chem. Acc.* **2006**, *115*, 100−112.

(26) Bock, C.; Kaufman, A.; Glusker, J. Coordination of Water to Magnesium Cations. *Inorg. Chem.* **1994**, *33*, 419−427.

(27) Spangberg, D.; Hermansson, K. Effective Three-Body Potentials for Li^+(aq) and Mg^{2+}(aq). *J. Chem. Phys.* **2003**, *119*, 7263−7281.

(28) Adrian-Scotto, M.; Mallet, G.; Vasilescu, D. Hydration of Mg^{+2}: a Quantum DFT and ab Initio HF Study. *THEOCHEM* **2005**, *728*, 231−242.

(29) Waizumi, K.; Masuda, I.; Fukushima, N. A Molecular Approach to the Formation of KCl and $MgCl^+$ Ion-Pairs in Aqueous Solution by Density Functional Calculations. *Chem. Phys. Lett.* **1993**, *205*, 317−323.

(30) Martinez, J. M.; Pappalardo, R. R.; Marcos, E. S. First-Principles Ion-Water Interaction Potentials for Highly Charged Monatomic Cations. Computer Simulations of Al^{3+}, Mg^{2+} and Be^{2+} in water. *J. Am. Chem. Soc.* **1999**, *121*, 3175−3184.

(31) Kortum, G.; Vogel, W.; Andrusson, K. *Dissociation Constants of Organic Acids in Aqueous Solution*; Butterworths: London, 1961.

(32) (a) Perrin, D. D. *Dissociation Constants of Organic Bases in Aqueous Solution*; Butterworths: London, 1965. (b) Perrin, D. D. *Dissociation Constants of Organic Bases in Aqueous Solution*, Supplement; Pergamon Press: NewYork, 1982.

(33) Davis, M. M. In *The Chemistry of Non-Aqueous Solvents*; Lagowski, J. J., Ed.; Academic: New York, 1970; Vol. 3.

(34) Arnett, E. M.; Scorrano, G. Protonation and Solvation in Strong Aqueous Acids. *Adv. Phys. Org. Chem.* **1976**, *13*, 83−153.

(35) (a) Taft, R. W. Kinetics of Ion−Molecule Reactions. *Prog. Phys. Org. Chem.* **1982**, *14*, 1. (b) Taft, R. W. In *Kinetics of Ion−Molecule Reactions*; Ausloos, P., Ed.; Plenum Press: New York, 1979. (c) Taft, R. W. In *Proton Transfer Reactions*; Caldin, E., Gold, V., Eds.; Chapman and Hall: London, 1975.

(36) Bower, M. T. *Gas Phase Ion Chemistry*; Academic Press: New York, 1979; Vol. 2.

(37) Yao-Chun, W.; Chuan, C.; Shin-Pon, J. Adsorption Mechanism and Dynamics Behavior of water and Ethanol Molecules inside Au Nanotubes. *Chin. J. Catal.* **2008**, *29*, 1099−1106.

(38) Gannon, G.; Larsson, J. A.; Greer, J. C.; Thompson, D. Guanidinium Chloride Molecular Diffusion in Aqeous and Mixed Water-Ethanol Solutions. *J. Phys. Chem. B* **2008**, *112*, 8906−8911.

(39) Turoverov, K. K.; Verkhusha, V. V.; Shavlovsky, M. M.; Biktashev, A. G.; Povarova, O. I.; Kuznetsova, I. M. Kinetics of Actin Unfolding Induced by Guanidine Hydrochloride. *Biochemistry* **2002**, *41*, 1014−1019.

(40) Sasahara, K.; Katsutoshi, N. Effect of Ethanol on Folding of Hen Egg-White Lysozyme Under Acidic Condition. *Proteins: Struc. Funct. Bioinf.* **2006**, *63*, 127−135.

(41) Hawlicka, E.; Rybicki, M. MD Simulation of the Ion Solvation in Methanol−Water Mixtures. In *Molecular Dynamics−Theoretical Developments and Applications in Nanotechnology and Energy*; Wang, L., Ed.; InTech: New York, 2012; Chapter 19.

(42) Hess, B.; Kutzner, C.; van der Spoel, D.; Lindahl, E. GROMACS 4: Algorithms for Highly Efficient, Load-Balanced, And Scalable Molecular Simulation. *J. Chem. Theory Comput.* **2008**, *4*, 435−447.

(43) Jorgensen, W. L.; Maxwell, D. S.; Tirado-Rives, J. Development and Testing of the Opls All-Atom Force Field on Conformational Energetics and Properties of Organic Liquids. *J. Am. Chem. Soc.* **1996**, *118*, 11225−11236.
(44) Jorgensen, W. L.; Chandrasekhar, J.; Madura, J. D.; Impey, R. W.; Klein, M. L. Comparison of Simple Potential Functions for Simulating Liquid Water. *J. Chem. Phys.* **1983**, *79*, 926−935.
(45) Tanaka, H.; Gubbins, K. E. Structure and Thermodynamics Properties of Water-Methanol Mixtures: Role of the Water-Water Interaction. *J. Chem. Phys.* **1992**, *97*, 2626−2634.
(46) Essmann, U.; Perera, L.; Berkowitz, M. L.; Darden, T.; Lee, H.; Pedersen, L. G. A Smooth Particle Mesh Ewald Method. *J. Chem. Phys.* **1995**, *103*, 8577−8593.
(47) Ryckaert, J. P.; Ciccotti, G.; Berendsen, H. J. Numerical Integration of the Cartesian Equations of Motion of a System with Constraints: Molecular Dynamics of n-Alkanes. *J. Comput. Phys.* **1977**, *23*, 327−341.
(48) Bussi, G.; Donadio, D.; Parrinello, M. Canonical Sampling through Velocity Rescaling. *J. Chem. Phys.* **2007**, *126*, 014101−014107.
(49) Berendsen, H. J. C.; Postma, J. P. M.; van Gunsteren, W. F.; DiNola, A.; Haak, J. R. Molecular Dynamics with Coupling to an External Bath. *J. Chem. Phys.* **1984**, *81*, 3684−3690.
(50) Parrinello, M.; Rahman, A. Polymorphic Transitions in Single Single Crystals: A New Molecular Dynamics Method. *J. Appl. Phys.* **1981**, *52*, 7182−7190.
(51) Nose, S.; Klein, M. L. Constant Pressure Molecular Dynamics for Molecular Systems. *Mol. Phys.* **1983**, *50*, 1055−1076.
(52) Pagnotta, S. E.; Ricci, M. A.; Bruni, F.; McLain, S.; Magazu, S. Water Structure around Trehalose. *Chem. Phy.* **2008**, *345*, 159.
(53) Ben-Naim, A. *Molecular Theory of Solution*; Oxford University Press: Oxford, New York, 2006.
(54) Martinez, L.; Andrade, R.; Birgin, E. G.; Martinez, J. M. *Packmole:* A Package for Building Initial Configurations for Molecular Dynamics Simulations. *J. Comput. Chem.* **2009**, *30*, 2157−2164.